Вестник Физико-технического института
Крымского федерального университета имени В. И. Вернадского
Том 1 (67–69). № 3. 2017. С. 23–37
Journal of Physics and Technology Institute of V. I. Vernadsky Crimean Federal University
Volume 1 (67–69). No. 3. 2017. P. 23–37

УДК 535.015

SIMPLE PHOTONICS CRYSTALS AS A MEDIUM FOR EXISTENCE OF OPTICAL QUARKS

Volyar A. V., Alexeyev C. N., Egorov Yu. A., Akimova. Ya. E.*

V. I. Vernadsky Crimean Federal University, Vernadsky Prospekt 4, Simferopol 295007, Russia
****E-mail:** yana_akimova_1994@mail.ru*

In this paper we demonstrated that in biaxial crystals under the condition of the conical diffraction the fractional-order vortices are unstable. We also demonstrated that the circular fiber array with a space-variant birefringence is an appropriate medium for fractional-order vortex beams in such arrays the supermodes may bear the half-integer order vortices in circular components. The decisive role in forming such supermodes plays evanescent-coupling assisted phase locking of individual fiber modes combined with tunneling of polarization states between anisotropic fibers in the array. We showed that integer-charge phase increment in a fractional-order supermode consists of two half-integer charge phase contributions. The implicit half-integer charge phase contribution (or the "hidden phase") comes due to the sign alteration of the amplitude factors in the field components that corresponds to the wavefront cuts. We have also made the comparison of the hidden and hydrodynamic phases in superfluidic fractional-charge vortices with analogous phases in fractional-order supermodes.

Keywords: optical vortices, fractional topological charges, the fractional-order supermodes, hidden phase, the array of optical vortices.

PACS: 41.85. –p

INTRODUCTION

In this paper we studied the shaping and evolution of singular beams bearing optical vortices with fractional topological charges both in uniform and non-uniform anisotropic media. Authors of the paper [3] remarked also unusual behavior of the orbital angular momentum l_z (OAM). At first glance it seems that the fractional-order vortex topological charge is an indicator of the OAM of singular beams at least records nearest values to its physical quantity. In some first papers ([7], [13]) authors obtained a nearly linear dependence between l_z and a topological charge p on the base of assessed theoretical results. However, the computer simulation of the process and physical analysis [12] revealed a complex behavior of the function $l_z(p)$. Small values of the charge $p < 10$ correspond to a nearly linear dependence l_z p with a small amplitude of oscillations. The growth of the value $p > 10$ results in increasing the amplitude of oscillations between the values $l_z = \mathrm{int}\,eger(p)$ and $p = 0$. The presented results are evidence of a complex interference coupling between a great number of the integer-order vortices in a fractional-order vortex beam.

One more unexpected property of the fractional-order vortex beams revealed the authors of the paper [15]. They tried to answer experimentally the question: can the fractional-order vortex beams control the states of the integer-order ones? They achieved a success using two beams: the pump and probe ones.

The pump beam is of a topological dipole field consisting of two ½- order vortices with opposite signs of their charges. The pump beam lays a course in a nonlinear medium for the probe singular beam of a smaller intensity. Changing parameters of the dipole they can steer the state of the probe beam. In fact, the fractional-order topological dipole is not destroyed inside the nonlinear medium forming the waveguide channel for the probe beam.

The example of structural stability of fractional-order vortex beams is a discrete fiber array with supermodes bearing half integer-order vortices [14].

1. THE SPACE VARIANT UNBOUNDED BIREFRINGENT MEDIUM

The brightest representatives of the space-variant media are the so-called q-plates [1]. The q-plate is, in the first version, a slab of a birefringent medium (liquid crystal) with different local directions of the crystal birefringence while the slab has uniform phase retardation. The space-variant birefringence of the q-plates is defined by the topological charge q equal to a rotation of the optical axis in a path circling around the plate center. Obviously, the value of q can be integer or half inter. The q – value can be controlled either by mechanical or by the electrical way ([2, 3]) that implements a polarization modulation at the input beam cross-section. The beam turns into a new wave state due to a superposition of a great number of plane waves with different polarization states. As a result the field distribution has a set of elliptic polarization states differ essentially from the birefringent structure of the q-plate.

There is not an appropriate physical mechanism in the device that could promote imprinting the space-variant birefringence structure into the propagating field. In that respect, the processes of the conical diffraction in the uniform biaxial crystal are not to differ from the effect of the q-plate. In essence, the main mechanism to construct the structured field in the q-plates are the superposition of the uniform propagating waves with the space-variant polarization far from that imprinted by the birefringent distribution of the anisotropic medium while the obtained wave construction maintains the desired fractional angular momentum. It means that the q-plate is solely destined for controlling the orbital angular momentum rather than for creating a stable fractional-order vortex-state.

At first sight it seems that the only physical mechanism of shaping the beams with the space-variant polarization in unbounded media is a superposition of the uniform propagating waves but for one little detail. The Fourier analysis is an appropriate approach only for unbounded media. However, such approach in the paraxial case cannot be applied to the wave beams in restricted media with a boundary surfaces where along with propagating waves exist non-radiative (*evanescent* [14]) waves.

One of such media is photonic crystal fibers that consist of a tightly compressed array of structured optical fibers. Their total birefringence is specified by the structure of a fiber stacking and local properties of single fibers [4–6]. The photonic crystals have two indefeasible advantages: the wave guiding property and the controlled fiber coupling. The simplest model of the photonic crystal is a discrete circular fiber array [7].

In the following section we will try to uncover basic physical processes responsible for the structural stability of vortex constructions with half integer-order topological

charges in non-uniform media with a discrete space-variant birefringence and the rules to form them integer-order vortex beams.

2. THE DISCRETE FIBER ARRAY: NON-ADIABATIC FOLLOWING AND OPTICAL QUARKS

A. Supermodes of anisotropic arrays

We will focus our attention on the discrete system of single mode birefringent fibers inserted into a transparent continuous medium with a uniform refractive index n_{cl} lesser than that of the fiber core $n_{co} < n_{cl}$ ([7–9]). Each optical fiber is located at the vertices of a regular *N*-gon as shown in Fig. 1. We will assume that the principal birefringence refractive indices n_e and n_o are such that $n_e \approx n_o \approx n_{co}$, $\delta n = n_{co} - n_{cl} << 1$ and $\Delta n = n_e - n_o << \delta n$.

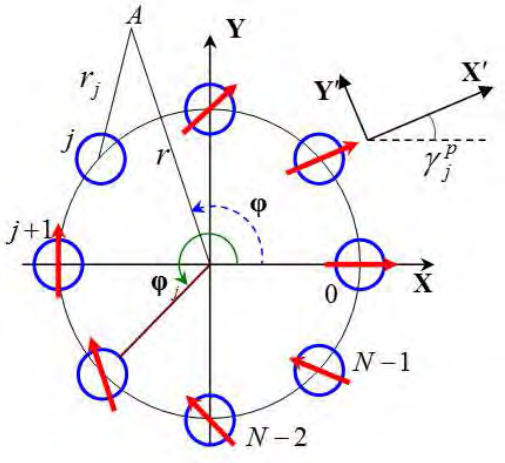

Fig. 1. Sketch of the birefringent fiber positions in the discrete circular fiber array

The principal point of our consideration is a distinctive distribution of the axes birefringence over the optical fibers: the birefringent directions at the $j-$ th fiber makes an angle γ_j^p with the X axis of the global frame

$$\gamma_j^p = \frac{2\pi\, p\, j}{N} = 2\varphi_p j, \quad \varphi_p = \frac{\pi}{N} p, \tag{1}$$

where $j = 0, 1, 2, \ldots N-1$ and p is a number of rotations of the fiber birefringence axis, i.e. the index p controls the position of the director of the anisotropic medium. The index $p = \left(2n_p + 1\right)/2, \quad n_p = 0, 1, 2, \ldots$ sets the characteristic index of the fiber array. The angle

φ_j points out the position of the local fiber in the array. Besides our consideration is restricted to the case of even N.

The fibers in the array are coupled due to a mutual penetration of the guided fields inside neighboring fibers. The coupling coefficient a (with the dimension m^{-2}) is general for all array and depends on the radius of the core. As a result, the coupled fiber modes form stable phase-locked field combinations (so-called super-modes) propagating with certain propagation constants. The field structure and the spectrum of their propagation constants are determined by the perturbation matrix [7]:

$$\hat{P} = a\cos 2\varphi_p \begin{pmatrix} 0 & 1 & 0 & ... & 0 & -1 \\ 1 & 0 & 1 & 0 & ... & 0 \\ 0 & 1 & 0 & ... & 0 & ... \\ ... & 0 & ... & ... & 1 & 0 \\ 0 & ... & 0 & 1 & 0 & 1 \\ -1 & 0 & ... & 0 & 1 & 0 \end{pmatrix}, \tag{2}$$

built through averaging over $X', Y'-$ polarized fundamental modes located at individual fibers. The mode spectrum P_v is found from the eigenvalue equation

$$\hat{P}\mathbf{K}_v = P_v\mathbf{K}_v \tag{3}$$

For the components K_v^j of the eigenvector $\mathbf{K}_v$ one has the following solution

$$K_v^j = \frac{\varepsilon^j}{\sqrt{N}}\exp\left(i\, j\, \varphi_{2m+1}\right), \tag{4}$$

The composite index v in (4) consists of two elements $v = (\varepsilon, m)$ so that its first element assumes two values: $\varepsilon = \pm 1$, $m = 0, 1, .. N/2-1$ and the eigenvalue read as

$$P_v = \varepsilon a\cos 2\varphi_p \cos\varphi_{2m+1}\ . \tag{5}$$

The expression for supermodes are built on the basis of the components K_v^j and are given by

$$\mathbf{X}_v = \sum_{j=0}^{N-1} K_v^j G_j \mathbf{i}'_j\ ,\quad \mathbf{Y}_v = \sum_{j=0}^{N-1} K_v^j G_j \mathbf{j}'_j\ , \tag{6}$$

where $\mathbf{i}'_j$, $\mathbf{j}'_j$ are the unit vectors directed along X', Y' axes associated with the $j-$ fiber. For the radial function we chose the Gaussian approximation [1]

$$G_j = E\exp\left(-\frac{r_j^2}{2w^2}\right), \tag{7}$$

where E is the field amplitude, w is the waist radius equal $w = \rho_0 / \sqrt{2\ln V}$, ρ_0 is the radius of the fiber core, $V = k\rho_0\sqrt{2\delta n}$, k is the wavenumber in free space.

The supermodes (51) are formed of fundamental modes of local fibers polarized along X', Y' local axes. The propagation constant $\beta_v^{x,y}$ of the $\mathbf{X}_v, \mathbf{Y}_v$ supermodes is given by [2]

$$\beta_v^{x,y} = \overline{\beta} + \frac{P_v}{2\overline{\beta}} \pm k\Delta n, \tag{8}$$

where $\overline{\beta}$ stands for the scalar propagation constant of each local fiber. The signs $(\pm)$ denote the upper indices in $\beta^{x,y}$, correspondingly.

Further we will analyze the supermode structure (6) in the circularly polarized basis. Thus, in the general case the mode field of each local mode is elliptically polarized so that the contributions to the *j*-th local fiber make the right-hand circular polarization in the form of the phase factor $\exp\left[i2\pi\, j\left(m - n_p\right)/N\right]$ and the left-hand one in the form of the $\exp\left[i2\pi\, j\left(m + n_p + 1\right)/N\right]$ factor. When we consider the array as a whole, the j index changes from 0 to $N-1$ so that the total increments of the phases over the vertices of the array are $2\pi\left(m - n_p\right)$ and $2\pi\left(m + n_p + 1\right)$. As we have in detail shown in [8] these increments from opposite circular polarizations set the *integer-order* vortex charge of the discrete fiber array. At first sight it seems that we can conclude that such fiber array *cannot* support the propagation of vortex modes with the fractional-order topological charges. However, we have showed in the first sub-section that fractional-order vortices can be formed by the superposition of the integer-order vortex modes. It proves also possible to form of the supermodes (4) the simple combinations that explicitly contain the circularly polarized components bearing the fractional-order vortex fields.

The basic point of our consideration lies in choosing the eigen modes bearing the fractional-order vortices. We can reach the desired results through combining the degenerated modes of the fiber array. In fact, the eigenvalues of the matrix $\hat{P}$ in (2) are double-degenerate because $P_{\varepsilon,m} = P_{-\varepsilon,N-2-m-1}$ (see eq. (5)) Since $\mathbf{K}^*_{\varepsilon,m} = \mathbf{K}_{-\varepsilon,N/2-m-1}$ it follows that $\mathbf{K}^*_v$ belongs to the same eigenvalues as $\mathbf{K}_v$. Further we have $\left(\mathbf{K}^*_v \cdot \mathbf{K}_v\right) = 0$, i.e. the vectors are linearly independent. Thus, we choose new set of eigenvectors in the form

$$\mathbf{e}_1 = \frac{\mathbf{K}_v - \mathbf{K}^*_v}{2i}, \quad \mathbf{e}_{-1} = \frac{\mathbf{K}_v + \mathbf{K}^*_v}{2}. \tag{9}$$

The new set of the eigenvectors can be conventionally divided into two parts with $\varepsilon = 1$ for the $\mathbf{e}_1$ eigenvectors and $\varepsilon = -1$ for $\mathbf{e}_{-1}$ ones. In accordance with eq. (2) we can obtain the alternative representation of the eigenvector components

$$\Gamma_v^j = \frac{1}{\sqrt{N}} \begin{cases} \sin\left(j\varphi_{2m+1}\right), \ \varepsilon = 1 \\ \varepsilon^j \cos\left(j\varphi_{2m+1}\right), \ \varepsilon = -1, \end{cases} \tag{10}$$

while the spectrum of the propagation constants remains defined by eq. (5) and the eigenvectors are recovered by replacement $K_v^j \to \Gamma_v^j$ in eq. (6). On the one hand, the function Γ_v^j is responsible for a number of zeros in eigen modes of the circular fiber array, but, on the other hand, the function Γ_v^j lodges the field zeros synchronously with the birefringence directions on the concrete local fibers in the array. We will call the fields with $\varepsilon = 1$ and $\varepsilon = -1$ the odd $\mathbf{E}_{o,m}$ and the even $\mathbf{E}_{e,m}$ mode beams, respectively.

For example, at $\varepsilon = 1$ for the amplitudes at the $j-th$ fiber for circular components of the $\mathbf{X}_v$ supermode we obtain $\exp\left(-2i\varphi_p j\right)\sin\left(\varphi_{2n+1} j\right)$ in the right circular polarization and $\exp\left(2i\varphi_p j\right)\sin\left(\varphi_{2n+1} j\right)$ in the left hand component. For the case $\varepsilon = -1$, the sines should be replaced multiplied by cosines multiple by the factor ε^{j-1}. In this case, the total phase increments in the components over the vertices of the array are $2\pi p$. In fact, the birefringence symmetry itself of the fiber array inserts the fractional-order topological charges p into supermode fields.

Following [3] we can write for the electric field components $E_v^{\pm}$ of the eigen supermodes:

$$E_v^{\pm}\left(r,\varphi,z\right) = G\sqrt{N}\sum_{j=0}^{N-1}\Gamma_v^j \exp\left[\frac{rr_0}{w^2}\cos\left(\varphi - 2\varphi_j\right) \quad 2ip\varphi_i - i\beta_v z\right], \tag{11}$$

where $G = E\exp\left[-\left(r^2 + r_0^2\right)/\left(2w^2\right)\right]$, r_0 is the array radius.

Typical field patterns on the background of the intensity distributions of the supermodes are shown in Fig. 2.

The pattern in Eq. 11, a has the C-shaped form where the electric field directed along the $\mathbf{X}'$ direction of the birefringence axis in each local fiber (see also Fig. 1) ($\left|1/2\right\rangle = E_{o,e}^{+}$). In the pattern in Fig. 2 b, the intensity distribution is the mirror-reflected intensity in Fig. 2 a.

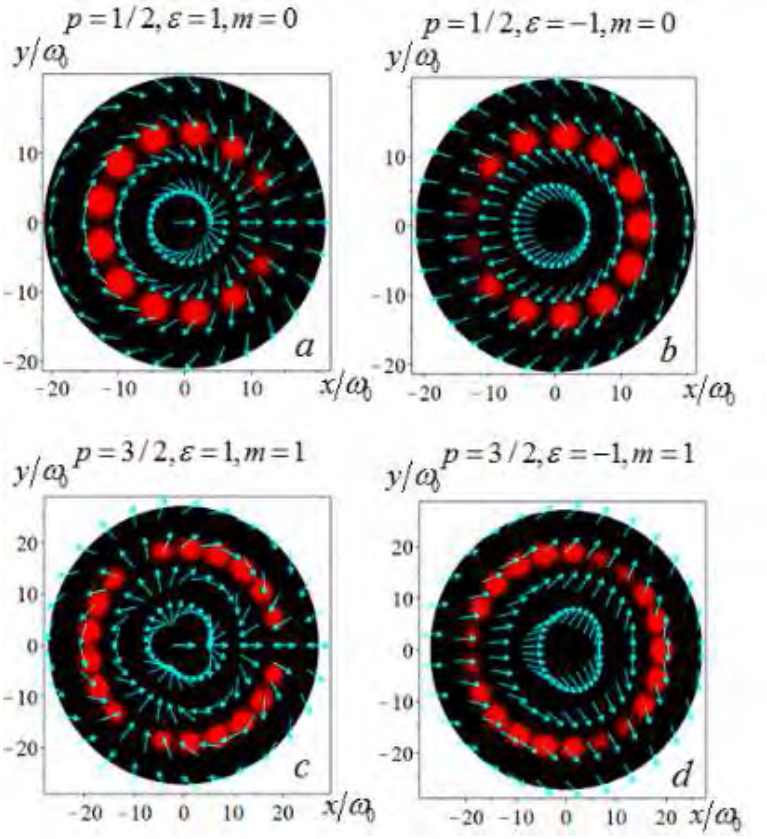

Fig. 2. The polarization and polarization distributions for the supermodes with $p = \pm 3/2$

However, the electric fields in each local fiber are directed along the $\mathbf{Y}'$ axis ($|-1/2\rangle = E_{o,e}^{-}$) under the condition that the fiber array index p remains the same (the local birefringent directions do not change). In accordance with the eq. (8) the propagation constants differ from each other by the value $\Delta\beta = \beta_{1,0} - \beta_{-1,0} = 2k\Delta n$. The patterns in Fig. 2 c and d have the mirror-reflected positions of the field zeros $(m = 1)$ but the fields in each local fiber are directed along the $\mathbf{X}'$ ($|3/2\rangle = E_{1,e}^{+}$) and $\mathbf{Y}'$ ($|-3/2\rangle = E_{1,e}^{+}$) axes, correspondingly. The difference between the propagation constants is $\Delta\beta = \beta_{1,1} - \beta_{-1,1} = 2k\Delta n$.

Curiously, the point $x = y = 0$ around which the full path-tracing is accorded by the rotation of the liner polarization by $\psi = \pi$ is not the singular point in a sense. The fact is that although the field has a space-variant linear polarization over all cross-section, the central point $x = y = 0$ cannot be related to any well-known polarization singularities.

Typical polarization singularities (star, lemon or monstar) imply the presence of the circular polarization at the center [9].

It is important to note that the local liner polarization in each eigen supermode of the fiber array follows the birefringence axes in the local fibers. Such optical phenomenon has much in common with the phenomenon of the adiabatic following in a twisted birefringent medium (in particular, in liquid crystals) [11]. In contrast to this classical effect, the matching of the field polarization and the fiber birefringence in the discrete fiber array is realized by jumps from one fiber to the other due to the mode coupling from the direction of neighboring fibers. In keeping with the adiabatic following phenomenon in the continuous anisotropic media we call the above effect the *non-adiabatic following* that underlies shaping all eigen supermodes in the discrete circular fiber array.

B. Is the "hidden phase" hidden indeed?

The following point of our treatment is to study the phase composition in the fractional-order vortex mode components. We plotted the phase patterns using the expressions (11) for the components of the vortex-beams shown in Fig. 3.

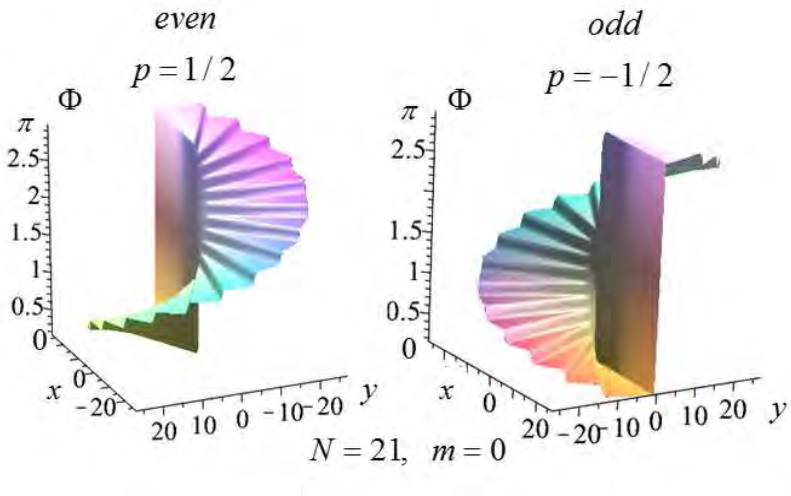

Fig. 3. The ladder-like phase patterns of the supermodes with $p = \pm 1/2$

One observes the ladder-like structure of the phase for the topological charges $p = \pm 1$ for the even and odd field components where the phase jump $\Delta\Phi = \pi$ is present at the center. However, in accordance with our notion in sub-section the fractional-order vortex beam is an infinite sum of the integer-order vortex beams. It is the set of integer-order vortices that makes up the phase deficiency $\Delta\Phi = \pi$. But we do not observe any traces of the integer-order vortices in Fig. 3.

Perhaps the presented plotting does not feel the hidden vortices? To answer this question and analyze the fine phase structure we studied the interference of the fractional beam with the plane and spherical waves. The interference patterns in Fig. 4 are formed

by the superposition of the odd $E_{o,0}^{+}$ component with the topological charge $p = 1/2$ and the plane (a) and spherical (b) waves.

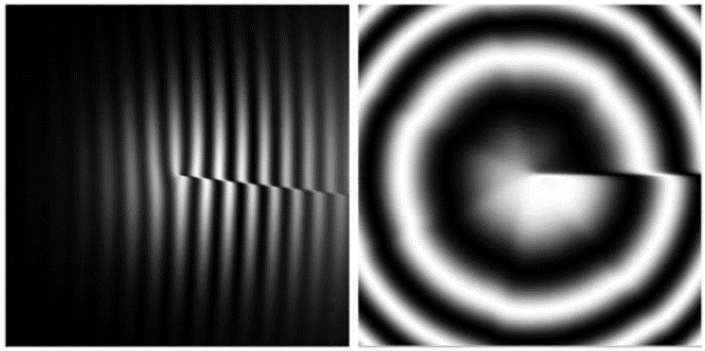

a *b*

Fig. 4. The interferential patterns of the $E_{o,0}^{+}$ component with $p = 1/2$

We observe again the ladder-like structure in the phase construction. There is only one broken fork at the end of the cut of the interference fringes (Fig. 4 a) and the cut of the interference spiral (Fig. 4 b) attesting to the phase jump π in the phase structure that resembles the ½-charged vortex imprinted in the field component. There are no any integer-order vortices in the patterns. Besides, such phase distribution preserves its structure when propagating along the fiber array in contrast to the fractional order vortex in free space that is ruined to an infinite number of integer-order vortices [12].

On the other hand, the overall phase increment of 2π, as should have been for a physical meaningful field, is composed of a continuous phase increment of π value which we attribute to a ½ - vortex charge and of a phase $\pi-$ jump at the cut of the wave front that preserves during the mode propagation in the wave guided medium. But such a treatment is only a simple explanation of the interference pattern without a successive physical mechanism that we will consider later on.

At first, let us show that the fractional-order vortex field component has no phase singularities. For this purpose, one can study the scalar optical current defined for a scalar field Ψ [13]

$$\mathbf{J} = i\left(\Psi\nabla_{\perp}\Psi^{*} - \Psi^{*}\nabla_{\perp}\Psi^{*}\right). \tag{12}$$

Taking into account eq. (11) and (12), one can obtain the expression for the transverse components of the optical current [13]

$$J_x - J_y \propto \sum_{n,m=0}^{N-1} \exp\left[2rr_0\cos\left(\varphi-\varphi_{m+n}\right)\cos\left(\varphi_{m-n}\right)/w^2\right]\sin\left(2p\varphi_{m-n}\right)\sin\varphi_n\sin\varphi_m \tag{13}$$

The summed expression in (13) is antisymmetric in m and n indices that gives $J_x = J_y$, i.e. the optical current does not contain vorticities. However, around the phase singularities the optical current should forms the closed trajectories [10]. Therefore, the circularly polarized component of the fractional-order vortex field (11) does not contain phase singularities.

C. Non-adiabatic following and optical quarks

The essential distinction between the continuous and discreet cases is that the smooth field distributions inside the optical fibers are broken by the gaps with other refractive indices and other field nature. In the continuous medium the only propagation wave participates in the transmitting process, at that the beam field of a unified infinite number of integer-order vortices at the initial plane scatters into an infinite number of self-dependent vortices. However, two waves – propagating and evanescent (arising at the refractive index gaps) influence the shaping supermodes of the discreet fiber array. Infinite number of the integer-order vortices in the supermode propagates as a single whole as if the vortices are glued together by the evanescent waves (the fiber coupling) along all length of the fiber array.

A part of the gluing between the fiber fields in the array plays *evanescent waves* [14] (a fiber coupling). It is the evanescent waves that are responsible for *the non-adiabatic following* effect shaping the extraordinary field structure different from that in other propagating fields in continuous media (e.g. in the conical diffraction processes in biaxial crystals and q-plates). The influence of the evanescent waves on the mode shaping falls into place if one imagines that the evanescent waves vanish in a blink. But then the wave guiding effect vanishes too and the supermode turns into an array of divergent light beams with a space-variant polarization so that we return to the q-plate case.

If we traverse around the array center at the radius r_0 (Fig. 2a) then the inclination angle of the linear polarization in each local fiber changes by jumps from 0 to π. Such a polarization evolution is mapped on the *Poincare sphere* as a motion along the equator. As a result, each component of the supermode (11) with the topological charge $p = 1/2$ acquires the *Pancharatnam–Berry phase* [15] $\phi_{PB} = \pi$ that is of the "hidden phase" considered above.

Let us consider a diagram representation of transmission of the vortex field with integer-order topological charges through a fiber array with half-integer-order index p presented in Fig. 5.

Case 1. Let the circularly polarized field with the integer order vortex charge $q = 1$ be formed at the input $z = 0$ of the array with the index $p = 1/2$. Naturally, we must expand the vortex state $|1\rangle$ over the eigen states $|1/2\rangle$ and $|-1/2\rangle$ propagating with their own propagation constants β_q and β_{-q} respectively.

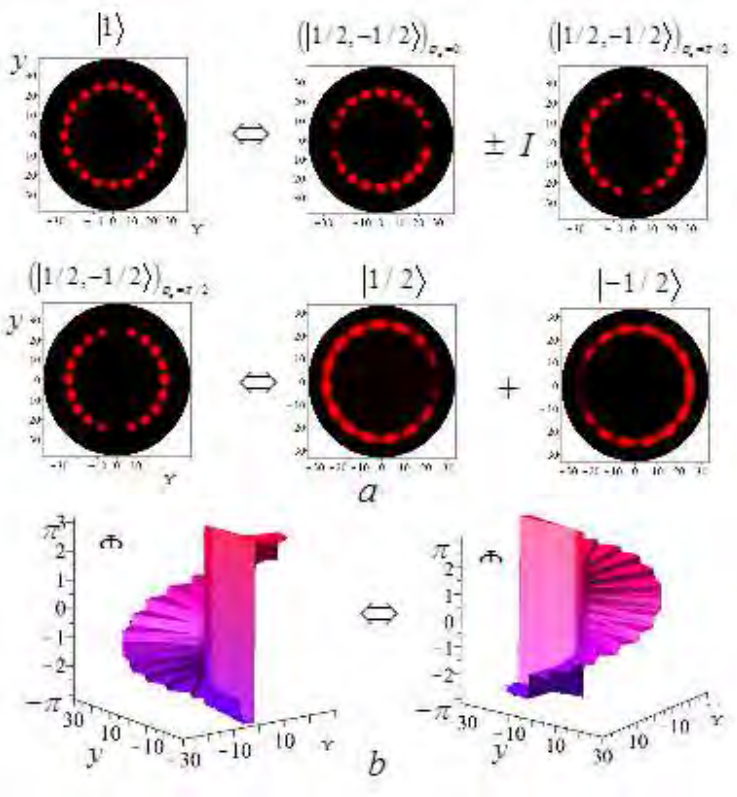

Fig. 5. Diagrams of the conversion of the $|1/2\rangle$ and $|-1/2\rangle$ supermode states

The first step to turn the initial vortex field into the topologically neutral one at the arbitrary array length consists in shaping the eigen supermodes $|q\rangle$ and $|-q\rangle$ into two the dipoles $\left(|1/2,-1/2\rangle\right)_{\varphi_0=0}$ and $\left(|1/2,-1/2\rangle\right)_{\varphi_0=\pi/2}$ rotated through an angle $\varphi_0=\pi/2$ with respect to each other (the first line in Fig. 5 a).

The second step is of their superposition with the phase shift $\pi/2$

$$|1\rangle \Rightarrow \begin{pmatrix} \cos\phi \\ i\sin\phi \end{pmatrix}\left[\left(|1/2,-1/2\rangle\right)_{\varphi_0=0} + I\left(|1/2,-1/2\rangle\right)_{\varphi_0=\pi/2}\right], \qquad (14)$$

where $\phi = k\Delta n\, z/2$. However, the second term in eq. (14) is nothing but than the sum of the odd and even states

$$\left(|1/2,-1/2\rangle\right)_{\varphi_0=\pi/2} \Rightarrow \left(|1/2,-1/2\rangle\right)^o + \left(|1/2,-1/2\rangle\right)^e. \qquad (15)$$

In turn, each topological dipole can be presented as a sum of two modes $|1/2\rangle$ and $|-1/2\rangle$ supermodes (the second line in Fig. 5 a). As far as the supermodes are transmitted

through the array with different propagation constants $\Delta\beta = \beta_{1/2} - \beta_{-1/2}$ we will observe the conversion of these states at the beating length $\Lambda = \pi / \Delta\beta$. The conversion of the integer-order states $|1\rangle e^{i\varphi} \Leftrightarrow |-1\rangle e^{-i\varphi}$ in the form of changing the phase starcase $\Phi(x, y)$ is shown in Fig. 5 b.

Case 2. Let the transverse electric field ($|TE\rangle$ mode state) be incident on the array input. The input field is of a superposition of two vortex constructions $|1\rangle e^{i\varphi}$, $|-1\rangle e^{-i\varphi}$ that have been regarded in Case 1. The state conversion develops in the frameworks of the above written diagram. We will observe the consecutive alternation of the $|TE\rangle$ and $|TM\rangle$ (transverse magnetic) states at the half-beating length $L_{b/2} = \dfrac{2\pi}{k\Delta n}$ shown in Fig. 5 whereas the conversion of the $|1/2\rangle \leftrightarrow |-1/2\rangle$ states take place at the length $L_{b/4} = \dfrac{\pi}{k\Delta n}$.

The detailed calculation shows ([1–8]) that if the projections of the electric field at the array input $z = 0$ onto the X', Y' local axes of the $j-th$ fiber are I_j and L_j, the amplitudes of the circularly polarized components $A_j^{\pm}$ at the $\alpha - th$ fiber in the global coordinates X, Y can be written as

$$A_\alpha^{\pm} = \sum_{v,j} K_v^{j*} K_v^{\alpha} \left(I_j e^{i\varphi} \quad iL_j e^{-i\phi} \right) e^{i\frac{\Delta\beta^2}{\beta} z \; i\gamma_\alpha^p}, \tag{16}$$

Let a right polarized field with the amplitude

$$A_j^{+} \propto \sin n\varphi_j \exp\left(-i2j\varphi_q\right), \tag{17}$$

where the indices $n-$ odd and $q-$ half-integer, be incident onto the fiber array with the index p. Then the field amplitude at the $z-$ section of the array is

$$\begin{aligned} A^{\pm} \propto G\sqrt{N} \sum_{\alpha=0}^{N-1} A_\varepsilon^{\pm} \exp\left[\frac{rr_0}{w^2} \cos\left(\varphi - 2\varphi_\alpha\right) \right] \times \\ \times \begin{pmatrix} \cos\phi \; e^{-i\alpha\varphi_{2q}} \\ i\sin\phi \, e^{i\alpha\varphi_{4p-2q-}} \end{pmatrix} \sin\left(\alpha\varphi_n - \frac{az}{\beta} \cos\varphi_{2p} \sin\varphi_{2p-2q} \sin\varphi_n \right) \end{aligned}. \tag{18}$$

In fact, the obtained equation is the analog of the expressions for the expansion into a series of the field with a fractional-order vortex fields over the integer-order ones in a continuous medium but for the fields in the discrete anisotropic media. When propagating the initial right hand polarized field with the fractional charge q induces the left hand polarized component with the fractional charge $2p - q$ modulated by the factor $\sin\phi$ while the right-hand polarization has the factor $\cos\phi$. Otherwise, we observe the energy

conversion along the array between the wave fields with the orthogonal circular polarizations but with different fractional topological charges.

Thus, the discrete fiber array with the inherent space-variant anisotropy is a particular medium for translating and preserving light fields with the fractional-order optical vortices. Any other fields bearing the integer-order vortices propagate through the array only as a superposition of the fractional-order eigen supermodes. After the fiber array, the supermode decays into many integer-order vortex beams.

From this point of view, we can regard the fractional vortex states $|p\rangle$ as *optical quarks* (predicted in [13]) similar to that in the Standard Model of particle physics, in particular, in the Gell-Mann's quark model of the hadrons [12]. The optical quarks in a free state can exist only inside the media with the inherent symmetry of the permittivity tensor. Out of the medium the optical quarks break up into the guided modes of the new optical structure.

CONCLUSION

We found that the space-variant birefringence with one singular point is inherent in the fractional-order vortex-beams at the crystals input under the condition of the conical diffraction. Typical scenario of the beam propagation here evolves in such a way that the topological charges of the fractional-order vortices in the circularly polarized components of vector beams differ from each other in one unit. The difference between the propagation constants of the components is independent on the value. It means that the biaxial crystal does not feel distinction between the fractional- and integer-order vortex beams. The same processes we observe also in the so-called q-plates, Moreover the polarization states at the beam cross-section are distributed by the complex way far from that of the birefringent directions in the crystal. Naturally the fractional-order vortex beams in the biaxial crystals and q-plates are also unstable one under propagation.

Quite another situation occurs in the discrete circular fiber array. The space variant birefringent axes in the fiber array are exactly recreated at the field cross-section. Such a polarization distribution is well preserved along all fiber array length in the form of a supermode. The shaping of the array eigen supermode is carried out due to the non-adiabatic following of the polarization states between the modes of the neighboring fibers when a linear polarization of different parts of the field follows strictly the birefringent axes of the local fibers. Thus, the fractional topological charge of the supermode is specified by the space-variant birefringence of a fiber array. A part of the "glue" of a great number of integer-order vortices into a single fractional-order one plays the evanescent waves between the local fibers.

We revealed a remarkable effect of shaping the integer-order vortex in a fiber array. Each integer-order vortex is of a superposition of four fractional order vortices with different propagation constants so that the integer-order mode decays and gathers together again along the array. We came to call them the optical quarks owing to resemblance of their behavior with that of quarks in the Standard Model of particle physics. The optical quarks can exist only inside the medium with an appropriate structural symmetry. Outside

the medium, the optical quarks are transformed into a cloud of standard integer-order vortices.

References

1. L. Marrucci, E. Karimi, S. Slussarenko, B. Piccirillo, E. Santamato, E. Nagali, F. Sciarrino, *J. Opt.* **13**, 064001 (2011).
2. S. Slussarenko, A. Murauski, T. Du, V. Chigrinov, L. Marrucci, E. Santamato, *Opt. Express* **19**, 4085–4090 (2011).
3. F. Cardano, E. Karimi, L. Marrucci, Corrado de Lisio, E. Santamato, *Opt. Express* **21**, 8815–8820 (2013).
4. T. Ritari, H. Ludvigsen, M. Wegmuller, M. Legré, N. Gisin, J. R. Folkenberg, M. D. Nielsen, *Opt. Express* **12**, 5943–5939 (2004).
5. A. Bezryadina, D. Neshev, A. Desyatnikov, J. Young, Z. Chen, Yu. Kivshar, *Opt. Express* **14**, 8317–8327 (2006).
6. S. Lee Yong, G. Lee Chung, Jung Yongmin, Oh Myoung-kyu, Kim Soeun, *J. Opt. Soc. Korea* **20**, 567–574 (2016).
7. C. N. Alexeyev, A. V. Volyar, M. A. Yavorsky, *Phys. Rev. A* **80**, 063821-12 (2009).
8. C. N. Alexeyev, A. O. Pogrebnaya, G. Milione, M. A. Yavorsky, *J. Opt.* **18**, 025602 (2016).
9. M. R. Dennis, *Opt. Commun.* **213**, 201–221 (2002).
10. M. V. Berry, *J. Opt. A* **11**, 094001 (2009).
11. A. Yariv, P. Yeh, *Optical waves in Crystals* (John Wiley & Sons, 1984), 102 p.
12. S. M. Wong, *Introductory Nuclear Physics* (Wiley Interscience Publication, 1998) 355 p.
13. A. V. Volyar, *Ukr. J. Phys. Opt.* **14**, 31–42 (2013).
14. Fornel F. de, *Evanescent waves* (Springer, Heidelberg, 2001) 111 p.
15. M. V. Berry, "Quantal Phase Factors Accompanying Adiabatic Changes", in *Proceedings of the Royal Society A* **392**, 45–57 (1984).

ПРОСТЫЕ ФОТОННЫЕ КРИСТАЛЛЫ КАК СРЕДСТВО СУЩЕСТВОВАНИЯ ОПТИЧЕСКИХ КВАРКОВ

Воляр А. В., Алексеев К. Н., Егоров Ю. А., Акимова Я. Е.*

Физико-технический институт, Крымский федеральный университет имени В. И. Вернадского, Симферополь 295007, Россия
E-mail: yana_akimova_1994@mail.ru

В настоящей работе показано, что в двухосных кристаллах при условии конической дифракции дробные вихри неустойчивы. Мы также продемонстрировали, что круговая волновая решетка с пространственно-вариантным двулучепреломлением является подходящей средой для вихревых пучков дробного порядка. В таких массивах супермоды могут иметь полуцелые порядковые вихри в круговых компонентах. Решающая роль в формировании таких супермод играет ускорение фазы синхронизации отдельных волоконных мод в сочетании с туннелированием состояний поляризации между анизотропными волокнами в массиве. Мы показали, что приращение фазы целочисленного заряда в супермоду дробного порядка состоит из двух вкладов фазы с половиной целого заряда. Неявный вклад фазы с полуцелой суммой (или «скрытая фаза») обусловлен изменением знака амплитудных коэффициентов в компонентах поля, соответствующих разрезам волнового фронта. Мы также провели сравнение скрытых и гидродинамических фаз

в сверхтекучих дробных вихрях с аналогичными фазами в супермодах дробного порядка.

Ключевые слова: оптически вихри, дробный топологический заряд, супермоды дробного порядка, скрытая фаза, массив оптических вихрей.

Список литературы

1. Spin-to-orbital conversion of the angular momentum of light and its classical and quantum applications / L. Marrucci, E. Karimi, S. Slussarenko, B. Piccirillo, E. Santamato, E. Nagali, F. Sciarrino // J. Opt., 2011. Vol. 13. 064001.
2. Tunable liquid crystal q-plates with arbitrary topological charge / S. Slussarenko, A. Murauski, T. Du, V. Chigrinov, L. Marrucci, E. Santamato // Opt. Express. 2011. Vol. 19. P. 4085–4090.
3. Generation and dynamics of optical beams with polarization singularities / F. Cardano, E. Karimi, L. Marrucci, Corrado de Lisio, E. Santamato // Opt. Express. 2013. Vol. 21, P. 8815–8820.
4. Experimental study of polarization properties of highly birefringent photonic crystal fibers / T. Ritari, H. Ludvigsen, M. Wegmuller, M. Legré, N. Gisin, J. R. Folkenberg, M. D. Nielsen // Opt. Express. 2004. Vol. 12, P. 5943–5939.
5. Observation of topological transformations of optical vortices in two-dimensional photonic lattices / A. Bezryadina, D. Neshev, A. Desyatnikov, J. Young, Z. Chen, Yu. Kivshar // Opt. Express. 2006. Vol. 14. P. 8317–8327.
6. Highly birefringent and dispersion compensating photonic crystal fiber based on double line defect core / Yong S. Lee, Chung G. Lee, Yongmin Jung, Myoung-kyu Oh, Soeun Kim // J. Opt. Soc. Korea. 2016. Vol. 20. P. 567–574.
7. Alexeyev C. N., Volyar A. V., Yavorsky M. A., Linear azimuthons in circular fiber arrays and optical angular momentum of discrete optical vortices // Phys. Rev. A. 2009. Vol. 80. 063821-12.
8. Propagation of light in a circular array of elliptical fibres / C. N. Alexeyev, A. O. Pogrebnaya, G. Milione, and M. A. Yavorsky // J. Opt. 2016. Vol. 18. 025602.
9. Dennis M. R., Polarization singularities in paraxial vector fields: morphology and statistics // Opt. Commun. 2002. Vol. 213. P. 201–221.
10. Berry M. V., Optical currents // J. Opt. A. 2009. Vol. 11. 094001.
11. A. Yariv, P. Yeh, Optical waves in Crystals // John Wiley & Sons. 1984. 102 p.
12. Wong S. M., Introductory Nuclear Physics // 2nd edition, Wiley Interscience Publication. 1998. 355 p.
13. Volyar A. V., Do optical quarks exist in free space? A scalar treatment // Ukr. J. Phys. Opt. 2013. Vol. 14. P. 31–42.
14. Fornel F. de, Evanescent waves // Springer, Heidelberg, 2001. 111 p.
15. Berry M. V., Quantal Phase Factors Accompanying Adiabatic Changes // Proceedings of the Royal Society A. 1984. Vol. 392, P. 45–57.

Поступила в редакцию 11.11.2017 г. Принята к публикации 22.12.2017 г.
Received November 11, 2017. Accepted for publication December 22, 2017